

Should sewage be discharged at the water surface or near the bed?

By RONALD SMITH

Department of Applied Mathematics and Theoretical Physics, University of Cambridge,
Silver Street, Cambridge CB3 9EW

(Received 30 March 1984 and in revised form 31 October 1984)

The mortality of bacteria in sewage discharges into shallow seas is strongly influenced by light and varies with distance from the free surface. Here a criterion is derived for deciding between the opposing strategies of getting rapid bacterial decay by directing the sewage up to the surface at the sacrifice of initial dilution, or of achieving high initial dilution with a distributed source along the bed perpendicular to the flow direction.

1. Introduction

In their forthcoming review article of dispersion in rivers and estuaries, Chatwin & Allen (1985) have drawn attention to the paucity of theoretical investigations either of non-conserved substance or of steady discharges. Many practical problems involve both these features, e.g. within the European Economic Community future coastal sewage discharges will have to be designed so that near designated bathing beaches the bacterial levels conform with an EEC directive (Commission of the European Communities 1976). The purpose of the present paper is to deal with this specific example and to incorporate the light (and hence depth) dependence of the bacterial mortality rate as pointed out by Gould & Munro (1981). Allowance is also made for a vertical drift velocity associated with buoyancy of the particles to which the bacteria are attached.

In the discussion of Gould & Munro's (1981) paper, there was controversy concerning the established practice of seeking high initial dilution, which means that in spite of any buoyancy the effective discharge level is very close to the bed (Anwar & Weller 1975). Munro pointed out that if one wants a lot of bacterial decay one should get the sewage on to the surface, even at the sacrifice of initial dilution. The results derived in the present paper quantify the choice facing the design engineer.

In keeping with the European orientation, the waters are considered to be relatively shallow and strongly tidal. For deeper or less strongly tidal waters, stratification can be important and the design considerations are different (Brooks 1960; Fischer *et al.* 1979, chapter 10; Roberts 1979).

2. Advection–diffusion equation

For steady discharges in flowing water, the contaminant plume is greatly elongated in the flow direction (see figure 5.6 of Fischer *et al.* 1979). Not only does this mean that longitudinal concentration gradients $\partial_x c$ are much smaller than transverse gradients $\partial_y c$, but also in the longitudinal direction the effects of diffusion are

overwhelmed by advection. Thus, in the advection–diffusion equation we retain transverse and vertical diffusion, but neglect longitudinal diffusion:

$$\alpha c + u \partial_x c + w \partial_z c = \kappa_2 \partial_y^2 c + \partial_z (\kappa_3 \partial_z c), \quad (2.1a)$$

$$\text{with} \quad wc - \kappa_3 \partial_z c = 0 \quad \text{on } z = 0, -h, \quad (2.1b)$$

$$\text{and} \quad uc = q \quad \text{at } x = 0. \quad (2.1c)$$

Here $\alpha(z)$ is the decay rate, $u(z)$ the longitudinal velocity, $w(z)$ the vertical drift velocity, $\kappa_2(z)$ the horizontal diffusivity, $\kappa_3(z)$ the vertical diffusivity, h the constant channel depth, and $q(y, z)$ the discharge flux at the effective source position $x = 0$. It is assumed that the contaminant plume is sufficiently dilute (i.e. the turbulence sufficiently strong) that the coefficients $\alpha, u, w, \kappa_2, \kappa_3$ are all independent of c .

In the absence of decay the equilibrium vertical concentration profile has the shape

$$\gamma(z) = \exp\left(\int_{z_0}^z \frac{w}{\kappa_3} dz'\right), \quad (2.2)$$

corresponding to a balance between vertical diffusion and vertical drift. For convenience we chose the reference level z_0 so that

$$\bar{\gamma} = 1, \quad (2.3)$$

where the overbar denotes the vertical average value. The non-uniform sampling of the velocity profile $u(z)$ means that, in the absence of decay, the effective advection velocity is given by

$$u_0 = \overline{u\gamma}. \quad (2.4)$$

As a temporary expedient, we simplify the vertical structure of the field equation (2.1a) by making the change of variables

$$c = \gamma^{\frac{1}{2}}(z) b(x, y, z). \quad (2.5)$$

The resulting equation for b does not have a $w \partial_z b$ term:

$$\left[\alpha + \frac{1}{2} \partial_z w + \frac{1}{4} \frac{w^2}{\kappa_3}\right] b + u \partial_x b = \kappa_2 \partial_y^2 b + \partial_z (\kappa_3 \partial_z b), \quad (2.6a)$$

$$\text{with} \quad \frac{1}{2} w b - \kappa_3 \partial_z b = 0, \quad \text{on } z = 0, -h, \quad (2.6b)$$

$$\text{and} \quad ub = \gamma^{-\frac{1}{2}} q \quad \text{at } x = 0. \quad (2.6c)$$

3. Eigenfunction expansion

To deal with the vertical structure of $b(x, y, z)$ we follow Noakes, McNulty & Wood (1984) and Smith (1982) and introduce the advection–diffusion eigenmodes $\phi_n(z)$:

$$\frac{d}{dz} \left(\kappa_3 \frac{d}{dz} \phi_n \right) + \left(\lambda_n u - \alpha - \frac{1}{2} \partial_z w - \frac{1}{4} \frac{w^2}{\kappa_3} \right) \phi_n = 0, \quad (3.1a)$$

$$\text{with} \quad \frac{1}{2} w \phi_n - \kappa_3 \frac{d\phi_n}{dz} = 0 \quad \text{on } z = 0, -h, \quad (3.1b)$$

$$\text{and} \quad \overline{u\phi_n^2} = u_0, \quad \overline{u\phi_n\phi_m} = 0 \quad \text{for } n \neq m. \quad (3.1c, d)$$

In the absence of decay the lowest mode is

$$\phi_0^{(0)} = \gamma^{\frac{1}{2}}(z), \quad \lambda_0^{(0)} = 0. \quad (3.2)$$

If we write
$$b = \sum_{n=0}^{\infty} b_n(x, y) \phi_n(z), \quad (3.3)$$

then we can replace the three-dimensional equations (2.6a-c) by a sequence of coupled two-dimensional equations

$$u_0(\partial_x b_n + \lambda_n b_n) = \sum_{m=0}^{\infty} \overline{\kappa_2 \phi_n \phi_m} \partial_y^2 b_m, \quad (3.4a)$$

with
$$u_0 b_n = \overline{q\gamma^{-\frac{1}{2}}\phi_n} \quad \text{at } x = 0. \quad (3.4b)$$

Fortunately, the vertical structure of $\kappa_2(z)$ closely resembles that of $u(z)$ (Fischer 1973, figure 3). Thus, in view of the orthogonality property (3.1d), we can approximate equations (3.4a, b) by the uncoupled equations

$$u_0(\partial_x b_n + \lambda_n b_n) = K_n \partial_y^2 b_n, \quad (3.5a)$$

with
$$u_0 b_n = \overline{q\gamma^{-\frac{1}{2}}\phi_n} \quad \text{at } x = 0, \quad (3.5b)$$

where
$$K_n = \overline{\kappa_2 \phi_n^2}. \quad (3.5c)$$

In particular, we note that in the absence of decay

$$K_0 = \overline{\kappa_2 \gamma}. \quad (3.6)$$

In the next section it is concluded that, away from the source, the b_0 contribution becomes dominant. Hence, an improvement upon (3.5a) would be to include the $\partial_y^2 b_0$ term

$$\begin{aligned} u_0(\partial_x b_n + \lambda_n b_n) - K_n \partial_y^2 b_n &= \overline{\kappa_2 \gamma^{\frac{1}{2}} \phi_n} \partial_y^2 b_0 \quad \text{for } n > 0 \\ &= \frac{\overline{\kappa_2 \gamma^{\frac{1}{2}} \phi_n}}{K_0} u_0(\partial_x b_0 + \lambda_0 b_0). \end{aligned} \quad (3.7)$$

The correction to b_n is small (but persistent) by virtue of the small value of the κ_2 integral and the small ratio λ_0/λ_n . Any systematic correction to the equation for b_0 would be correspondingly small.

4. Hermite series solution

At large distances downstream the transverse concentration profile becomes Gaussian. A particularly economical method for representing the approach to normality is by means of a Hermite series (Chatwin 1970):

$$b_n = \frac{Q_n}{hu_0} \frac{\exp(-\lambda_n x - \frac{1}{2}\eta^2)}{(2\pi)^{\frac{1}{2}}\sigma} \left\{ 1 + \sum_{m=3}^{\infty} q_{nm} \left(\frac{\sigma(0)}{\sigma}\right)^m \text{He}_m(\eta) \right\}, \quad (4.1a)$$

with
$$Q_n = \int_{-\infty}^{\infty} h \overline{q\gamma^{-\frac{1}{2}}\phi_n} dy, \quad \eta = \frac{y - Y_n}{\sigma}, \quad (4.1b, c)$$

and
$$\sigma^2 = \sigma^2(0) + \frac{2K_n x}{u_0}. \quad (4.1d)$$

Here Q_n is the component of the total contaminant flux associated with the n th mode, Y_n is the centroid of the initial discharge, and $\sigma^2(0)$ the initial variance. The

higher-order coefficients q_{n3}, q_{n4} relate to the skewness and kurtosis (spikiness) of the initial discharge:

$$Q_n q_{nm} = \frac{1}{m!} \int_{-\infty}^{\infty} h q \gamma^{-\frac{1}{2}} \overline{\phi_n} \text{He}_m(\eta) dy. \tag{4.2}$$

The first few Hermite polynomials are:

$$\text{He}_0 = 1, \quad \text{He}_1 = \eta, \quad \text{He}_2 = \eta^2 - 1, \quad \text{He}_3 = \eta^3 - 3\eta, \quad \text{He}_4 = \eta^4 - 6\eta^2 + 3. \tag{4.3}$$

The conventional ordering

$$0 \leq \lambda_0 < \lambda_1 < \lambda_2 < \dots \tag{4.4}$$

of the eigenvalues means that, on the lengthscale $1/(\lambda_1 - \lambda_0)$ of vertical mixing, the concentration will be dominated by the lowest mode

$$c \approx \gamma^{\frac{1}{2}}(z) \phi_0(z) b_0(x, y). \tag{4.5}$$

In practice this would be on a lengthscale of about 40 water depths downstream (Smith 1979). In shallow European coastal waters, this is very close to the discharge.

Similarly, on a lengthscale of $\sigma^2(0) u_0 / 2K_n$ the detailed transverse character of the initial discharge becomes unimportant, and the series (4.1a) is dominated by the first term. In shallow water with

$$\kappa_2 \approx 0.2hu_*, \quad u_*/u_0 \approx 0.05 \tag{4.6}$$

(Fischer 1973, figure 3 and table 1), this lengthscale is

$$x > \frac{50\sigma^2(0)}{h}. \tag{4.7}$$

Commonly the discharge is distributed over a cross-flow distance greater than the water depth. Thus, the condition (4.7) tends to be more stringent than that for the neglect of the higher modes.

The resulting asymptote for the concentration is given by

$$c = \frac{\exp(-\lambda_0 x - \frac{1}{2}\eta^2) \gamma^{\frac{1}{2}}(z) \phi_0(z)}{hu_0 [2\pi(\sigma^2(0) + 2K_0 x/u_0)]^{\frac{1}{2}}} Q_0, \tag{4.8a}$$

with

$$\eta = \frac{y - Y}{[\sigma^2(0) + 2K_0 x/u_0]^{\frac{1}{2}}}, \tag{4.8b}$$

and

$$Q_0 = \int_{-\infty}^{\infty} h q \gamma^{-\frac{1}{2}} \overline{\phi_0} dy. \tag{4.8c}$$

In the absence of decay $\phi_0^{(0)} = \gamma^{\frac{1}{2}}$ and Q_0 is the total flux of contaminant into the flow. However, when there is decay, the amplitude Q_0 of the lowest mode depends both upon the total flux and upon the discharge height.

5. Design criterion

Whenever possible sewage works, and the associated sewage outfalls, are not situated in high-amenity areas. Thus, there is a considerable distance along the flow direction before criteria such as the EEC directive become operative. Hence, we can use (4.8a) to predict a maximum surface concentration

$$c_{\max} = \frac{\exp(-\lambda_0 x) \gamma^{\frac{1}{2}}(0) \phi_0(0) Q_0}{hu_0 [2\pi(\sigma^2(0) + 2K_0 x/u_0)]^{\frac{1}{2}}}. \tag{5.1}$$

When the total contaminant flux is specified

$$Q = \int_{-\infty}^{\infty} \int_{-h}^0 q \, dy \, dz, \quad (5.2)$$

and when there is no decay ($Q_0 = Q$), the only way a design engineer can influence c_{\max} is via the initial lateral spread $\sigma(0)$. However, when there is decay there is the second possibility of reducing Q_0 by changing the discharge height. In particular, for a surface discharge with small $\sigma^2(0)$, we have

$$c_{\max} = \frac{\exp(-\lambda_0 x) \phi_0(0)^2 Q}{h u_0 [4\pi K_0 x / u_0]^{\frac{1}{2}}}. \quad (5.3)$$

Provided that (5.3) conforms to (say) the EEC directive at the downstream distance x of the high-amenity region, we have a choice of discharge strategies. A bottom discharge,

$$Q_0 = \gamma^{-\frac{1}{2}}(-h) \phi_0(-h) Q \quad (5.4)$$

with large $\sigma^2(0)$, has high initial dilution and will have lower concentrations for small x . The narrow surface discharge has an increased mortality rate of the bacteria, exposed to the stronger light intensity near the surface. The consequent reduced value of Q_0 ,

$$Q_0 = \gamma^{-\frac{1}{2}}(0) \phi_0(0) Q, \quad (5.5)$$

leads to lower concentrations at large x . The transition point when the values of c_{\max} are equal is given by

$$\frac{\sigma^2(0)}{h^2} = \frac{x}{h} \frac{2K_0}{h u_0} \left[\frac{\phi_0(-h)^2}{\gamma(-h)} \frac{\gamma(0)}{\phi_0(0)^2} - 1 \right]. \quad (5.6)$$

If we specify the distance x of a high-amenity area, then (5.6) gives the minimum lateral spread $\sigma(0)$ for it to be worthwhile having a distributed bottom-discharge.

6. Weak decay

If the decay lengthscale $1/\lambda_0$ were comparable with the decay lengthscale $40h$ of the higher modes (Smith 1979), then the exponential decay in (5.1) would render the bacterial level negligible comparatively close to the discharge. Thus, it is reasonable to regard the α and λ_0 terms in (3.1a) as small perturbations.

We denote the $\alpha = 0$ modes and eigenvalues by $\phi_n^{(0)}$, $\lambda_n^{(0)}$ and we represent ϕ_0 as a perturbation about $\phi_0^{(0)} = \gamma^{\frac{1}{2}}$:

$$\phi_0 = \gamma^{\frac{1}{2}}(z) + \sum_{n=1}^{\infty} a_n \phi_n^{(0)}(z) + \text{second-order terms.} \quad (6.1)$$

This series automatically satisfies the boundary conditions (3.1b). The field equation (3.1a) becomes

$$(\lambda_0 u - \alpha) \gamma^{\frac{1}{2}} - \sum_{n=1}^{\infty} \lambda_n^{(0)} a_n u \phi_n^{(0)} = \text{second-order terms.} \quad (6.2)$$

Making use of the orthogonality properties (3.1c, d) of the $\phi_n^{(0)}$ modes, we infer that to the first approximation

$$\lambda_0 = \frac{\overline{\alpha \gamma}}{u_0}, \quad a_n = -\frac{\overline{\alpha \gamma^{\frac{1}{2}} \phi_n^{(0)}}}{\lambda_n^{(0)} u_0}. \quad (6.3a), (6.3b)$$

The crucial measure (5.6) of the respective performance of bottom and surface discharges can be related to a source-height function $S(z)$:

$$\frac{\sigma^2(0)}{h^2} = 4\lambda_0 x[S(-h) - S(0)]. \tag{6.4}$$

From the above representation (6.1, 6.3) for ϕ_0 and the formula (5.6), we can infer that $S(z)$ has the series representation

$$S(z) = -\left(\frac{K_0}{hu_0}\right) \gamma^{-\frac{1}{2}}(z) \sum_{n=1}^{\infty} \frac{\alpha\gamma^{\frac{1}{2}}\phi_n^{(0)}}{h\lambda_n^{(0)}\alpha\gamma} \phi_n^{(0)}(z). \tag{6.5}$$

The presence of the eigenmodes $\phi_n^{(0)}$ makes this result appear impractically complicated. However, if we now reverse the transformation (2.5) between (2.1a) and (2.6a), we discover that $\gamma S(z)$ is the solution of the vertical diffusion equation

$$w \frac{d(\gamma S)}{dz} - \frac{d}{dz} \left(\kappa_3 \frac{d(\gamma S)}{dz} \right) = \frac{K_0}{h^2} \left[\frac{u\gamma}{u\gamma} - \frac{\alpha\gamma}{\alpha\gamma} \right], \tag{6.6a}$$

with $w\gamma S - \kappa_3 \frac{d\gamma S}{dz} = 0$ at $z = 0, -h,$ (6.6b)

and $\overline{u\gamma S} = 0.$ (6.6c)

This last condition (6.6c) corresponds to the absence of $\phi_0^{(0)}(z)$ in the series (6.5). Equations (6.6a-c) can be solved without recourse to the use of eigenmode expansions.

7. The source-height function

Invoking a mathematical trick repeatedly used by Smith (1981, §5), we write the first integral of (6.6a, b):

$$\frac{dS}{dz} = -p_+(z) \frac{K_0}{\kappa_3 \gamma h^2} \int_{-h}^z \left(\frac{u\gamma}{u\gamma} - \frac{\alpha\gamma}{\alpha\gamma} \right) dz' + p_-(z) \frac{K_0}{\kappa_3 \gamma h^2} \int_z^0 \left(\frac{u\gamma}{u\gamma} - \frac{\alpha\gamma}{\alpha\gamma} \right) dz', \tag{7.1a}$$

where $p_+ + p_- = 1.$ (7.1b)

At this stage the splitting (7.1b) can be arbitrary. However, the form of the condition (6.6c) makes it expedient for us to choose

$$p_+(z) = \frac{1}{h} \int_z^0 \frac{u\gamma}{u\gamma} dz', \quad p_-(z) = \frac{1}{h} \int_{-h}^z \frac{u\gamma}{u\gamma} dz'. \tag{7.2a, b}$$

Hence the notation p_+, p_- relates to the upper and lower boundaries respectively.

Preserving the symmetry with respect to the two boundaries, we find that the source-height function has the explicit solution

$$S(z) = \frac{K_0}{h^2} \int_z^0 \frac{p_+(z')}{\gamma\kappa_3} \left[\int_{-h}^{z'} \left(\frac{u\gamma}{u\gamma} - \frac{\alpha\gamma}{\alpha\gamma} \right) dz'' \right] dz' + \frac{K_0}{h^2} \int_{-h}^z \frac{p_-(z')}{\alpha\kappa_3} \left[\int_{z'}^0 \left(\frac{u\gamma}{u\gamma} - \frac{\alpha\gamma}{\alpha\gamma} \right) dz'' \right] dz'. \tag{7.3}$$

Moreover, the choice (7.2a, b) of p_+, p_- ensures that this solution does indeed satisfy the condition (6.6c) as well as (6.6a, b). Conveniently, only the first integral contributes to $S(-h)$, and only the second integral to $S(0)$. After minor simplification we arrive at the expression

$$S(-h) - S(0) = \frac{K_0}{h^2} \int_{-h}^0 \frac{1}{\gamma\kappa_3} \int_{-h}^z \left(\frac{u\gamma}{u\gamma} - \frac{\alpha\gamma}{\alpha\gamma} \right) dz' dz. \tag{7.4}$$

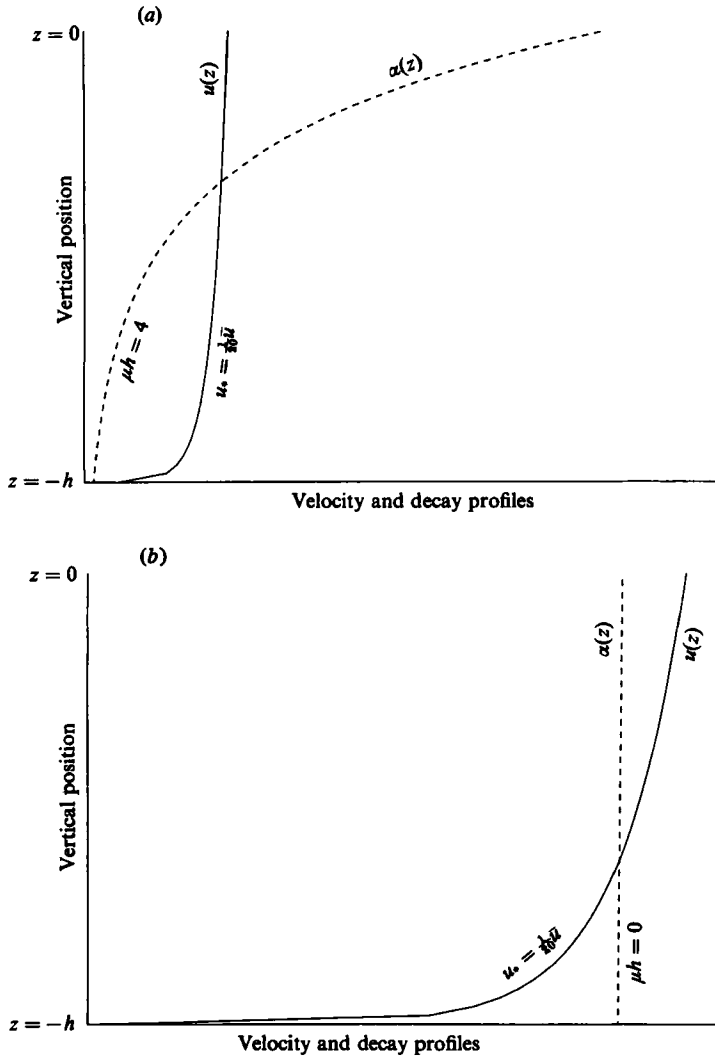


FIGURE 1. Relative shapes of the vertical profiles of velocity $u(z)$ and decay rate $\alpha(z)$ for cases in which (a) a surface discharge is effective, and (b) a bottom discharge is best.

This factor in the design criterion

$$\left(\frac{\sigma(0)}{h}\right)^2 = 4x\lambda_0[S(-h) - S(0)], \tag{7.5}$$

depends upon the relative shapes of the velocity and decay profiles. For a case such as illustrated in figure 1 (a), the inner integral in (7.4) is positive. Thus, in accord with the work of Gould & Munro (1981), we find that at large distances a bottom discharge would need to be sufficiently wide in order to achieve the same concentration as from a narrow surface discharge. Conversely, a radio-active discharge with α independent of z (see figure 1 b) is best discharged at the bed. In one case the dominant physical effect is the enhanced decay rate near the surface, while in the other it is the small extra amount of time taken for the radio-active contaminant to diffuse into the faster-moving part of the flow.

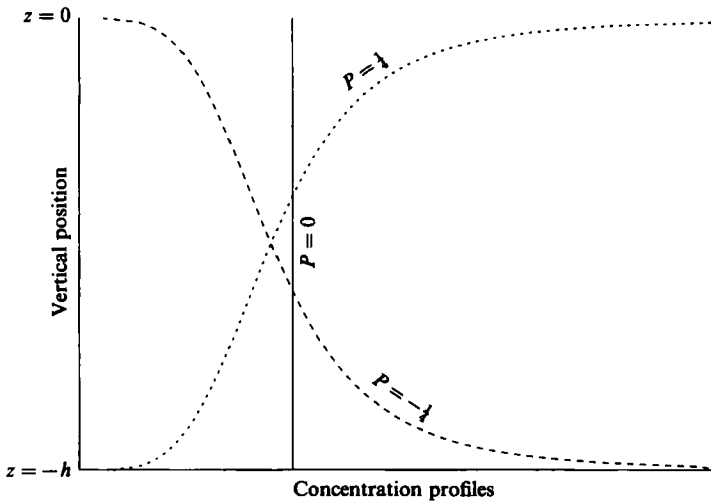


FIGURE 2. The equilibrium concentration profile $\gamma(z)$ in neutral —; upward drift; and downward drift --- cases.

8. Illustrative example

To utilize the above analyses we first require the vertical profiles of $\alpha, u, w, \kappa_2, \kappa_3$. Then we can evaluate the sequence (2.2), (2.3), (2.4), (3.6), (6.3a), (7.4) of integrals for $\gamma(z), u_0, K_0, \lambda_0$ and $[S(-h) - S(0)]$. Motivated by figure 4 of Gould & Munro (1981) and figures 2 and 3 of Fischer (1973), we consider the idealized case

$$\left. \begin{aligned} \alpha &= \hat{\alpha} \exp(\mu z), & u &= \bar{u} + \frac{u_*}{k} \left[1 + \ln \left(1 + \frac{z}{h} \right) \right], \\ w &= \text{constant}, & \kappa_2 &= \frac{1}{2} k h u_* (1 + z/h)^{1/2}, \\ \kappa_3 &= k h u_* \left(1 + \frac{z}{h} \right) \left(-\frac{z}{h} \right), & u_* &= 0.05 \bar{u}, \\ k &= 0.4. \end{aligned} \right\} \quad (8.1a-g)$$

Here $\hat{\alpha}$ is the peak mortality rate as experienced at the free surface, μ the light attenuation rate below the surface, u_* friction velocity at the bed, and k is von Kármán's constant. Although the functional forms of u and κ_2 are not identical, the logarithmic and power-law profiles are very similar in shape (as noted in §3).

The equilibrium vertical concentration profile is given by

$$\gamma = \frac{1}{\Gamma(1+P)\Gamma(1-P)} \left[\frac{z+h}{z} \right]^P, \quad \text{with } P = \frac{w}{k u_*}, \quad (8.2a, b)$$

where Γ denotes the Gamma function (Abramowitz & Stegun 1974, chapter 6). For non-zero P there is the unrealistic feature of weak singularities at one of the boundaries (see figure 2). This can be removed if κ_3 is kept non-zero. However, in the subsequent analysis only integrals are required, and the singularities can be tolerated provided that $|P| < 1$. Indeed, the logarithmic velocity profile (8.1b) has a negative (reversed flow) singularity at the bed, yet nevertheless is widely used because of its modelling of gross features.

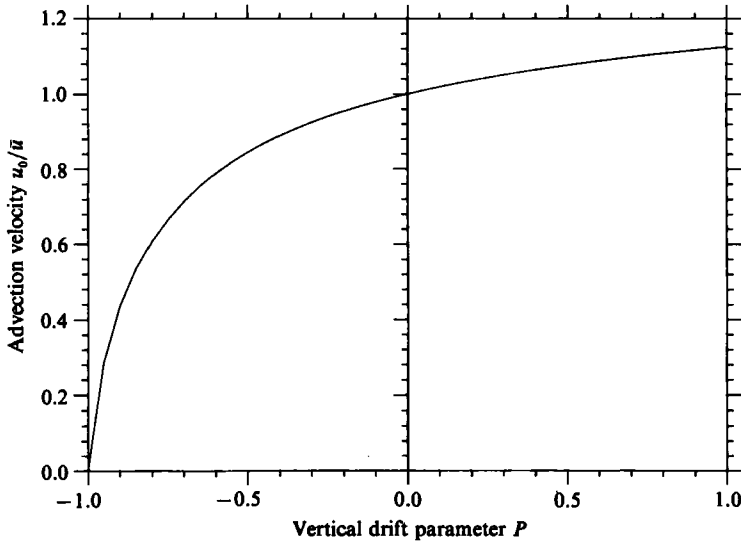


FIGURE 3. The dependence of the contaminant advection velocity $u_0 = \overline{u\gamma}$ as a function of the vertical drift parameter $P = w/ku_*$.

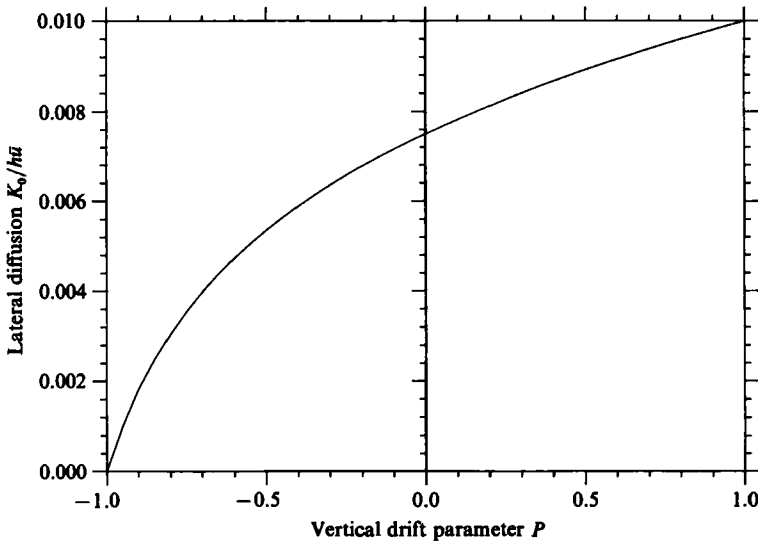


FIGURE 4. The dependence of the effective transverse diffusivity $K_0 = \overline{\kappa_2 \gamma}$ of the contaminant upon the vertical drift parameter $P = w/ku_*$, with $u_* = \frac{1}{20}\bar{u}$.

The velocity shear is significant only very close to the bed. Thus, the weighted average advection velocity u_0 differs little from the bulk fluid velocity \bar{u} unless there is a marked downwards drift (see figure 3). Similarly, the weighted average transverse diffusivity K_0 varies most markedly near $P = -1$ (see figure 4).

Figure 5 shows the horizontal decay rate λ_0 as a function of the light attenuation rate μh for three values of P . As we might expect, the sensitivity to the light attenuation is greater when there is downwards drift and the contaminant tends to be away from the strongly lit surface layers.

Finally, figure 6 gives graphs of the shape factor $[S(-h) - S(0)]$ for the same three

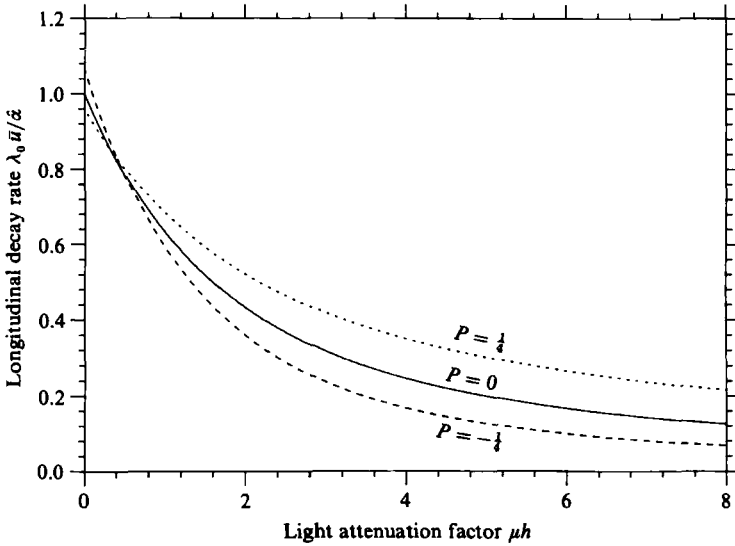


FIGURE 5. The horizontal contaminant decay rate $\lambda_0 = \overline{\alpha\gamma}/\overline{u\gamma}$ as a function of the light attenuation factor μh in neutral —; upward drift; and downward drift --- cases.

values of P . As was noted in the previous section, there is a change of sign near $\mu h = 0$. Even in clear water the e folding depth for light is only about 1.5 m. Thus, in practice, the shape factor is positive. The larger values of the shape factor when P is negative conforms with the physical argument that when the bacteria tend to sink there is a greater premium upon the initial enhanced mortality rate associated with a surface discharge.

As a quantitative example for the application of the design criterion (7.5), we specify

$$\left. \begin{aligned} P = 0, \quad \hat{\alpha} = 1.66 \times 10^{-3} \text{ s}^{-1}, \quad h = 5 \text{ m}, \quad \mu h = 4, \\ \bar{u} = 0.1 \text{ m s}^{-1}, \quad x = 10^3 \text{ m}. \end{aligned} \right\} \quad (8.3)$$

Hence there are neutrally buoyant bacteria, in bright (English summer) sunlight (Gould & Munro 1981, figure 2), discharged into clear water with depth 5 m and with current velocity 0.1 m s^{-1} . The high-amenity region is only 1 km downstream of the discharge. From figure 5 we can deduce that the horizontal decay rate is given by

$$\lambda_0 = 0.25 \frac{\hat{\alpha}}{\bar{u}} = 4.2 \times 10^{-3} \text{ m}^{-1}, \quad (8.4)$$

and from figure 6 we find

$$S(-h) - S(0) = 0.55. \quad (8.5)$$

The criterion (7.5) for the equal performance of surface and bottom discharges yields

$$\left(\frac{\sigma}{h}\right)^2 = 4x\lambda_0[S(-h) - S(0)] = 9.24, \quad \sigma = 15 \text{ m}. \quad (8.6)$$

Equivalently, a uniform bottom discharge of total length $2\sqrt{3}\sigma = 52 \text{ m}$ would be required. The magnitude of the transitional discharge length in this example shows the practical importance of the question of discharge design raised by Gould & Munro (1981).

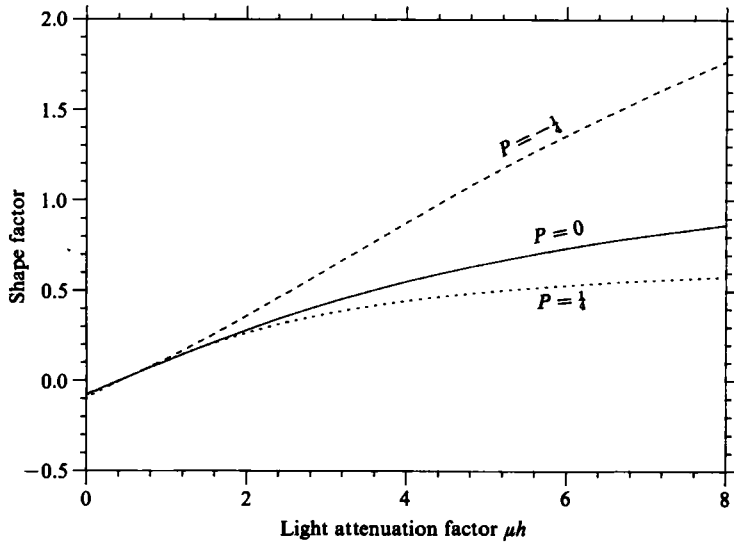


FIGURE 6. The shape factor $[S(-h) - S(0)]$ as required in the design criterion (7.5) for the relative performance of surface and bottom discharges.

It happens that if the bacteria were attached to particles with a rise velocity of $0.5 \times 10^{-3} \text{ m s}^{-1}$ (i.e. $P = \frac{1}{4}$), then the increased mortality rate

$$\lambda_0 = 0.34 \frac{\hat{\alpha}}{\bar{u}} \quad (8.7)$$

is almost exactly counterbalanced by the decreased shape factor

$$S(-h) - S(0) = 0.45, \quad (8.8)$$

leaving the transition value for σ virtually unchanged. Similar cancelling occurs if the particles sink. To a lesser extent, there is also insensitivity to the light attenuation rate. What is important is the peak mortality rate $\hat{\alpha}$. The stronger the sunlight the larger the transitional value of σ . Thus, the relative performance of a surface discharge is best just when it is needed most: when bright sunlight brings holiday-makers (with their extra sewage burden) to the seaside and into the water.

The author wishes to acknowledge the financial support of the Royal Society, and the considerable stimulus of hearing a lecture by Dougal Munro of the Water Research Centre, Stevenage.

REFERENCES

- ABRAMOWITZ, M. & STEGUN, I. A. 1964 *Handbook of Mathematical Functions*. Dover.
- ANWAR, H. O. & WELLER, J. A. 1975 Experiment on submarine outfall of slot type discharging into a cross flow. *Report No. INT 143, Hydraulics Research Station, Wallingford*.
- BROOKS, N. H. 1960 Diffusion of sewage effluent in an ocean current. In *Proc. 1st Int. Conf. on Waste Disposal in the Marine Environment, July 1959* (ed. E. A. Pearson), pp. 246–267. Pergamon.
- CHATWIN, P. C. 1970 The approach to normality of the concentration distribution of a solute in a solvent flowing along a straight pipe. *J. Fluid Mech.* **43**, 321–352.

- CHATWIN, P. C. & ALLEN, C. M. 1985 Mathematical models of dispersion in rivers and estuaries. *Ann. Rev. Fluid Mech.* **17** (to appear).
- COMMISSION OF THE EUROPEAN COMMUNITIES 1976 Council Directive of 8 December 1975 concerning the quality of bathing water. *Official Journal No. L31*, 5 February.
- FISCHER, H. B. 1973 Longitudinal dispersion and turbulent mixing in open channel flow. *Ann. Rev. Fluid Mech.* **5**, 59-78.
- FISCHER, H. B., LIST, E. J., KOH, R. C. Y., IMBERGER, J. & BROOKS, N. H. 1979 *Mixing in Inland and Coastal Waters*. Academic.
- GOULD, D. J. & MUNRO, D. 1981 Relevance of microbial mortality to outfall design. *Coastal Discharges*, pp. 45-50. Thomas Telford: London.
- NOAKES, R. I., McNULTY, A. J. & WOOD, I. R. 1984 Turbulent dispersion from a steady two-dimensional horizontal source. *J. Fluid Mech.* **149**, 147-159.
- ROBERTS, P. J. W. 1979 Line plume and ocean outfall dispersion. *J. Hydraul. Div., ASCE* **105**(HY4), 313-331.
- SMITH, R. 1979 Calculation of shear dispersion coefficients. *Mathematical Modelling of Turbulent Diffusion in the Environment*, pp. 343-362. Academic.
- SMITH, R. 1981 The importance of discharge siting upon contaminant dispersion in narrow rivers and estuaries. *J. Fluid Mech.* **108**, 43-53.
- SMITH, R. 1982 Where to put a steady discharge in a river. *J. Fluid Mech.* **115**, 1-11.